

time scale observed in some close binary systems (19), and tidal dissipation (20) may also cause a white dwarf to spiral into a red giant on a time scale short enough to be important in this phase.

Mass transfer continues at an accelerating rate during this stage (phase IV) of orbital contraction, and the massive, degenerate helium core of star A continues to grow. It is not clear whether neutrino losses in this phase are sufficient to prevent helium ignition. Even if helium ignition does occur, however, it is unlikely that the radius of the helium core will expand enough to fill its Roche lobe, and the core temperature certainly remains much too low for carbon ignition to occur (21).

We are thus led to a situation in which star A is ultimately pushed over the Chandrasekhar limit by continued accretion of the mass transferred back from star B. At this stage (phase V), the masses of the two stars are $M_A^{(V)} \sim 1.4 M_\odot$, $M_B^{(V)} \sim M_A^{(I)} + M_B^{(I)} - 1.4 M_\odot$ ($\sim 1.6 M_\odot$); star A is a massive, degenerate white dwarf; star B is evolving toward the red-giant phase and has a degenerate helium core of mass $\sim 0.1 M_B^{(II)}$ ($\sim 0.3 M_\odot$). At this stage, the core of star A undergoes collapse, and the residual nuclear fuel is ignited to power a supernova explosion.

Most of the energy released in a supernova event is carried off by neutrinos and is unavailable for ejecting mass from the star (22). If a few tenths of a solar mass are ejected with velocities $\sim 10^4$ km sec $^{-1}$, as is typical of type I supernovas, the energy content of the ejecta is $\sim 10^{50}$ ergs. If the radius of the star at the time of the supernova explosion of star A is $\sim 0.5 R_\odot$, compared to a separation of $\sim R_\odot$, then star B subtends a fractional solid angle $\Delta\Omega/4\pi \sim 0.1$. The energy absorbed by the envelope of star B from the expanding supernova shell is thus $\sim 10^{49}$ ergs, and this is sufficient to eject virtually the entire hydrogen envelope of star B, leaving only the residual helium core with a mass of perhaps $\sim 0.2 M_B^{(II)}$ ($0.6 M_\odot$) in orbit around the pulsar remnant of mass $\sim 1.2 M_\odot$. From Fig. 1 we note that this particular set of parameters is just excluded by the orbital kinematics, but qualitatively similar systems (for example, a $0.7 M_\odot$ companion and a $0.98 M_\odot$ pulsar or a $0.8 M_\odot$ companion and a $1.2 M_\odot$ pulsar) are entirely possible. The observations thus appear to be entirely compatible with this evolutionary scheme.

On the basis of the analysis presented in this report, we conclude that two of the most important observational programs that should be carried out are (i) the measurement of the long-term average \dot{P} and

(ii) a search for a radio SNR at the position of the pulsar. We are of course aware that both tidal and general relativistic effects will be important in this system, but a discussion of these effects is beyond the scope of the report. It is clear, however, that this system will be a veritable laboratory for both gravitational theories and the study of neutron star structure.

H. M. VAN HORN
S. SOFIA*, M. P. SAVEDOFF
J. G. DUTHIE
R. A. BERG

Department of Physics and Astronomy
and C. E. Kenneth Mees Observatory,
University of Rochester,
Rochester, New York 14627

References and Notes

1. J. H. Taylor and R. A. Hulse, *Int. Astron. Union Circ. 2704* (4 Oct. 1974); R. A. Hulse and J. H. Taylor, *Astrophys. J.* **195**, L51 (1975).
2. J. P. Ostriker and J. E. Gunn, *Astrophys. J.* **157**, 1395 (1969).
3. J. M. Comella, H. D. Croft, R. V. E. Lovelace, J. M. Sutton, *Nature (Lond.)* **221**, 453 (1969).
4. M. I. Large, A. E. Vaughan, R. Wielebinski, *ibid.* **220**, 754 (1968).
5. W. J. Cocke, M. J. Disney, D. J. Taylor, *ibid.* **221**, 525 (1969).

6. G. J. Fishman, F. R. Harnden, R. C. Haymes, *Astrophys. J.* **156**, L107 (1969).
7. R. Giacconi, S. Murray, H. Gursky, E. Kellogg, E. Schreier, T. Matilsky, D. Koch, H. Tananbaum, *Astrophys. J. Suppl. Ser.* **27**, 37 (1974).
8. B. Margon and A. Davidsen, *Int. Astron. Union Circ. 2712* (24 Oct. 1974).
9. G. Baym, C. Pethick, P. Sutherland, *Astrophys. J.* **170**, 299 (1971).
10. Z. Kopal, *Close Binary Systems* (Wiley, New York, 1959).
11. C. W. Allen, *Astrophysical Quantities* (Athlone, London, 1963).
12. S. Van den Bergh, A. P. Marscher, Y. Terzian, *Astrophys. J. Suppl. Ser.* **26**, 19 (1973).
13. D. K. Milne, *Aust. J. Phys.* **23**, 425 (1970); D. Downes, *Astron. J.* **76**, 305 (1971).
14. R. Kippenhahn, K. Kohl, A. Weigert, *Z. Astrophys.* **69**, 265 (1968).
15. R. P. Kraft, *Astrophys. J.* **135**, 408 (1962); B. Warner and R. E. Nather, *Mon. Notic. R. Astron. Soc.* **152**, 219 (1971).
16. P. Giannone and A. Weigert, *Z. Astrophys.* **67**, 41 (1967).
17. W. K. Rose, *Astrophys. J.* **152**, 245 (1968).
18. S. Starrfield, W. M. Sparks, J. W. Truran, *ibid.* **192**, 647 (1974); *Astrophys. J. Suppl. Ser.* **28**, 247 (1974).
19. J. Faulkner, *Astrophys. J.* **170**, L99 (1971).
20. W. M. Sparks and T. P. Stecker, *ibid.* **188**, 149 (1974).
21. G. Shaviv and N. Vidal, *Astrophys. Space Sci.* **15**, 195 (1972); T. J. Mazurek, *ibid.* **23**, 365 (1973).
22. S. A. Colgate and R. H. White, *Astrophys. J.* **143**, 626 (1966).
23. This work was supported in part by the National Science Foundation under grant MPS 74-13257.

* On leave from the Astronomy Department, University of South Florida, Tampa 33620.

29 November 1974; revised 14 March 1975

Laser Raman Spectroscopy—New Probe of Myosin Substructure

Abstract. *Laser Raman spectroscopy is used to probe the heterogeneous substructure of the large contractile protein myosin. Some peaks are assigned to specific chemical groups of the molecule; others, notably the conformationally sensitive amide III vibrations, provide information on the structurally distinct regions of the molecule. Deuteriation of the NH groups is instrumental in the assignment of these vibrational modes. The relative intensities of bands typical of α -helical conformations (near 1265 and 1304 cm^{-1}) and bands associated with nonhelical structure (near 1244 cm^{-1}) are sensitive indicators of myosin substructure and represent potentially useful probes of conformational changes.*

Myosin, one of the chief constituents of the contractile apparatus of muscle (and other motile systems), accounts for approximately half of myofibrillar protein. Myosin contains two α -helical heavy chains ($\sim 200,000$ daltons each) twisted around each other to form a long coil (Fig. 1a); each heavy chain terminates in a globular head portion (1, 2). Most of the long coil portion can be isolated by limited tryptic digestion of myosin (3, 4) as the light meromyosin. Each globular head portion is associated with two small peptide chains ($\sim 20,000$ daltons each) and contains functionally important sites for interactions with actin and adenosine triphos-

phate (5). Such interactions associated with conformational changes (5, 6) of myosin are considered to play a crucial role in the molecular mechanism underlying muscle contraction.

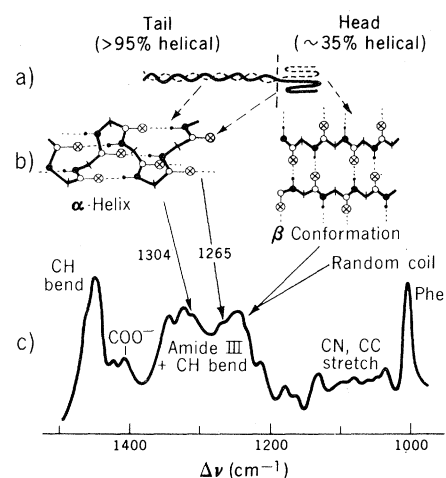


Fig. 1. One possible correlation of (a) the structurally distinct subregions of myosin, (b) their proposed conformational structures, and (c) the Raman spectrum of the amide III region of myosin. Arguments favoring this interpretation of the spectral results are presented in the text.

This report concerns the first application of laser Raman spectroscopy to myosin; it suggests that Raman spectroscopy will prove useful in the investigation of physiologically significant conformational changes of myosin. This prospect is strengthened by very recent studies of conformational changes induced by heat and Mg^{2+} (7, 8) as well as studies of myosin subfragments (9). While laser Raman spectroscopy has been employed to study simple molecules [for example, ionophores (10, 11), homopeptides (12, 13), and small proteins (14-16)], it has not previously been used to investigate proteins of the size and structural heterogeneity of myosin.

Laser Raman spectroscopy is particularly useful for studies of proteins in aqueous solution since the incident and detected radiation are both visible light (water strongly absorbs infrared radiation, thereby limiting similar application of infrared spectroscopy). In Raman experiments, one illuminates a sample with an intense beam of monochromatic light of frequency ν_{laser} and detects scattered light of various frequencies ν_i produced by inelastic scattering in the sample. The frequency shifts $\Delta\nu \equiv \nu_{\text{laser}} - \nu_i$, commonly termed Raman frequencies, correspond to

normal vibrational modes associated with characteristic motions of diatomic or polyatomic groups of the scattering molecules.

The peptide "amide modes," which involve nitrogen vibrations, are particularly sensitive to molecular conformation. The amide I mode (with a Raman frequency near 1650 cm^{-1}) represents $\text{NC}=\text{O}$ stretch vibrations, while the amide III mode (1220 to 1320 cm^{-1}) is associated with coupled CN stretch and NH in-plane bending vibrations (17).

Our Raman spectra are taken on a Spex Ramalog 4 system using a Spectra-Physics model 164 Ar^+ laser. The response of the thermoelectrically cooled RCA-31034 photomultiplier (GaAs photocathode) is essentially flat between 4000 and 7000 \AA . The laser output is passed through a Claassen filter to eliminate plasma lines. A quartz wedge polarization scrambler placed before the entrance slit of the spectrometer assures equal instrumental response to all polarizations of the scattered light. The samples are held in Kimax glass capillary tubes (inner diameter, 1 mm) mounted perpendicular to the scattering plane. Incident power levels of 100 to 400 mw and spectral resolutions of 4 to 6 cm^{-1} are sufficient for our purposes. All Raman

frequencies are calibrated to the vibrations of CCl_4 .

The myosin used was extracted from freshly excised rabbit psoas muscle by the method of Nauss *et al.* (18), except that a second dilution in $0.06M$ KCl was substituted for $(\text{NH}_4)_2\text{SO}_4$ precipitation. The concentration of isolated myosin was usually 10 mg/ml ($\sim 20\text{ }\mu\text{M}$) and was increased two to five times by dialysis against starch (or occasionally sucrose) followed by dialysis overnight against $0.6M$ KCl , $\text{pH } 7.0$. The resulting solution was centrifuged at $100,000g$ for 1 hour to remove any remaining actomyosin, polymyosin, or denatured myosin. Samples strictly prepared in this manner gave reproducible results.

The amide III region of myosin is shown in Fig. 2a; for comparison, aqueous solutions of amino acids at relative concentrations corresponding to their content in myosin (19) are also shown (Fig. 2, b to d). The amino acid spectra between 1230 and 1320 cm^{-1} lack the intense activity apparent in myosin near 1240 and 1310 cm^{-1} . The 1244 cm^{-1} band of myosin may correspond to either β structure or random coil conformations, or to a mixture of both (in particular, the 1232 cm^{-1} shoulder may correspond to β structure). In contrast, no

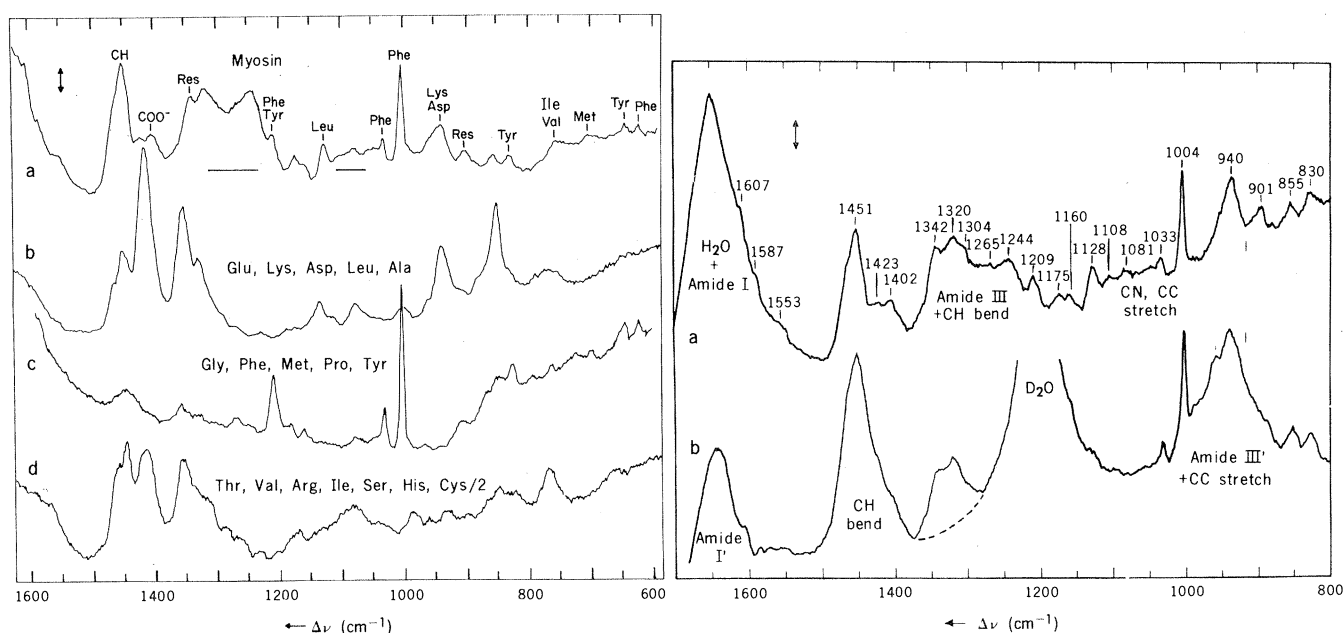


Fig. 2 (left). Comparison of Raman spectra of aqueous solutions of myosin (a) and its constituent amino acids (b to d). The relative concentrations of the amino acids correspond to those in myosin (19). The five most prevalent amino acids appear in (b); those in (c) are most common in the globular head portions of the myosin molecule. Horizontal lines indicate regions containing contributions from vibrations near the peptide bond. Abbreviations: Res, residue vibration; Gly, glycine; Thr, threonine; Ser, serine; Ile, isoleucine; His, histidine; Cys/2, cystine; other abbreviations and more complete assignments appear in Table I. Conditions were: (a) myosin, 35 mg/ml in $0.6M$ KCl , $\text{pH } 7.0$; (b, c, and d) amino acids, $\text{pH } 6.0, 3.0,$ and 11.0 , respectively (to aid solution). Resolution, 5 cm^{-1} ; scanning speed, $30\text{ cm}^{-1}/\text{min}$; vertical arrow, 300 count/sec in (a) and 3000 count/sec in (b to d); laser power, 600 mw in (a) and 200 mw in (b to d); excitation, 5145 \AA . Fig. 3 (right). Comparison of Raman spectra of myosin in (a) H_2O and (b) D_2O solution ($0.6M$ KCl , $\text{pH } 7.0$). Solvent peaks occur in different regions in these solvents (near 1650 and 1200 cm^{-1} , respectively). Deuteration of the NH groups of myosin shifts the amide III activity from the region 1220 to 1320 cm^{-1} to the region 890 to 990 cm^{-1} . The decrease in intensity from 1240 to 1310 cm^{-1} in D_2O solution verifies the presence of amide III contributions in that region in spectra of normal myosin. Spectral resolution, 5 cm^{-1} ; scanning speed, (a) $30\text{ cm}^{-1}/\text{min}$ and (b) $60\text{ cm}^{-1}/\text{min}$; vertical arrow, 300 count/sec ; laser power, 500 mw ; excitation, 5145 \AA .

α -helical polypeptides are known to display amide III frequencies below 1260 cm^{-1} .

Our interpretations (shown in Table 1 and Fig. 1) are based in part upon data from simpler molecules. Generally, β structure is expected to appear between 1225 and 1240 cm^{-1} , whereas random coil conformations appear between 1235 and 1250 cm^{-1} . For example, the β conformations of poly-L-valine (12), polyglycine I (20), and poly-L-lysine (13) have amide III frequencies at 1229, 1234, and 1240 cm^{-1} , respectively, whereas the random coil conformations of glucagon, insulin, and poly-L-glutamic acid (16) have amide III frequencies at 1235, 1239, and 1248 cm^{-1} , respectively.

The shoulder at 1265 cm^{-1} as well as the shoulder at 1304 cm^{-1} are at frequencies typical of α -helical structure (12-16, 20); comparison with the Raman spectra of myosin subfragments (9) suggests that these peaks are associated with at least two structurally distinct α -helical parts of the myosin molecule. The 1265 cm^{-1} shoulder appears to be associated with the globular α -helical fraction, while the fibrous α -helical conformation of myosin is dominant in the 1304 cm^{-1} region (Fig. 1).

Our interpretation of the 1265 cm^{-1} myosin band is supported by comparison with the 1262, 1265, and 1266 cm^{-1} amide III frequencies of α -helical lysozyme (15), poly-L-alanine (12), and glucagon (16), respectively. Higher amide III frequencies are observed in poly- γ -benzyl-L-glutamate (12) and poly- γ -methyl-L-glutamate (21) (1294 and 1300 cm^{-1} , respectively). CH bending modes contribute heavily to the region 1320 to 1360 cm^{-1} (compare Fig. 2, b to d) and, in general, deuteration is required to authenticate amide frequencies.

The substitution of D_2O for H_2O (Fig. 3) shifts the solvent peak from $\sim 1650 \text{ cm}^{-1}$ to $\sim 1200 \text{ cm}^{-1}$, which greatly improves visibility in the amide I region (1620 to 1680 cm^{-1}). Deuteration of the NH groups of myosin by dissolving it in a solution of KCl in D_2O dramatically affects the region 1220 to 1320 cm^{-1} , shifting amide III vibrations $\sim 300 \text{ cm}^{-1}$ downward in frequency. The decrease in Raman activity near 1244, 1265, and 1304 cm^{-1} in deuterated myosin (Fig. 3b) identifies the missing portions of those bands as amide III vibrations; a similar reduction in the relative intensity of the 1304 cm^{-1} band occurs in depolarized Raman spectra. We believe this polarized, deuteration-sensitive portion of that band to be an α -helical amide III vibration, whereas the remaining unaffected portion may represent CH bending modes. A prominent peak at 1306 cm^{-1} appears in

Table 1. Raman frequencies of myosin. Notation: sh, shoulder; and (), frequency uncertain. Abbreviations: Phe, phenylalanine; Tyr, tyrosine; Met, methionine; Lys, lysine; Val, valine; Asp, aspartic acid; Leu, leucine; Glu, glutamic acid; Arg, arginine; and Pro, proline.

Peak (cm^{-1})	Tentative assignment
622	CC ring twist (Phe)
645	CC ring twist (Tyr)
660 to 695	CS vibrations
704	CS stretch (Met)
755	Amide V; residue vibrations
780	
830	CC symmetric ring stretch (Tyr)
855	CH_2 residue rock (especially Tyr)
(882)	
901	CC residue stretch
940	CC residue stretch (Lys, Asp); CH_3 symmetric stretch (Leu, Val)
(962)sh	CH_3 symmetric stretch
1004	CC ring stretch (Phe); weak CC stretch (Lys, Glu)
1033	CC ring bend (Phe)
(1044)?	CH_2 twist (Glu, Arg, Pro)
(1058)?	CH_2 twist (Lys, Arg); CH, CC stretch (?)
1081, 1104	CN, CC skeletal stretch
1128	Isopropyl residue antisymmetric stretch; CN stretch (?)
1160, 1175	CH_3 antisymmetric rock (Leu, Val); CH rock (Phe, Tyr)
1209	Tyr, Phe modes
1244	Amide III (β chain + random coil)
(1265)sh	Amide III; CH bend (Leu, Asp, Glu, Tyr, Pro)
(1304)sh, 1320	Amide III (α -helix); CH bend, CH_2 twist
1342	CH bend (especially residue)
1402	COO^- symmetric stretch (Asp, Glu)
1423	Residue vibration (Asp, Glu, Lys)
1451	CH_3 (antisymmetric), CH_2 , CH bend
1553	Amide II; COO^- antisymmetric stretch (Asp)
1587	Phe, Arg vibrations
1607	Phe, Tyr ring vibrations
1650	H_2O , amide I regions

Raman spectra of the light meromyosin subfragment of myosin (9), which is more than 95 percent α -helical. Subtraction of spectra in D_2O from spectra in H_2O , with due consideration of differing Raman scattering efficiencies, could permit an estimate of the relative amounts of α , β , and random coil structures in myosin; such a procedure has been applied with limited success to several other proteins (22).

Changes in myosin structure are reflected in the Raman spectra. For example, increasing the temperature from 20° to 68°C increases the intensity of the 1244 cm^{-1} band (random coil or β structure), as might be expected on denaturation.

We have focused attention on the amide III region because of its usefulness as a conformational indicator. Other portions of myosin's Raman spectrum are similarly useful, although not as readily interpretable. For example, thermal denaturation of myosin also leads to changes in the region 1040 to 1120 cm^{-1} , which contains conformationally sensitive skeletal vibrations (mostly CN and CC stretch modes). Similar modes appear in the Raman spectra of lysozyme (15), ribonuclease (14), and α -poly-L-lysine (13). In contrast, the ring vibrations of phenylalanine (strong near 1004, 1033, and 1209 and

weak near 622, 1587, and 1607 cm^{-1}), and tyrosine (strong at 1209, a doublet near 830 and 850, and weak near 645 cm^{-1}) are relatively insensitive to environment.

The CS stretch modes of myosin appear near 704 cm^{-1} (methionine residue) and 669 and 693 cm^{-1} (disulfide linked). Similar peaks occur near 668 and 678 cm^{-1} in insulin (16), 661 and 700 cm^{-1} in lysozyme (15), and 696 cm^{-1} in dimethyl sulfide (15). Vibrations of the ionized COO^- groups of the aspartic and glutamic acid residues account for the peaks at 1402 cm^{-1} (symmetric stretch) and 1533 cm^{-1} (antisymmetric stretch). The majority of the remaining peaks represent CC and CH vibrations of the amino acid residues; these appear in the component spectra of Fig. 2, b to d.

The ability of Raman spectroscopy to probe chemically and structurally distinct portions of the myosin molecule suggests its potential utility in investigating physiologically interesting processes.

E. BAYNE CAREW, IRVIN M. ASHER
H. EUGENE STANLEY

Harvard-MIT Program in Health
Sciences and Technology and
Department of Physics,
Massachusetts Institute of Technology,
Cambridge 02139

References and Notes

1. S. Lowey, H. S. Slayter, A. G. Weeds, H. Baker, *J. Mol. Biol.* **42**, 1 (1969).
2. L. C. Gershman, A. Stracher, P. Dreizen, *J. Biol. Chem.* **244**, 2726 (1969); J. Gazith, S. Himmelfarb, W. F. Harrington, *ibid.* **245**, 15 (1970).
3. E. Mihalyi and A. G. Szent-Gyorgyi, *ibid.* **201**, 189 (1953).
4. J. Gergely, M. A. Gouvea, D. Karibian, *ibid.* **212**, 165 (1955).
5. "The mechanism of muscle contraction," *Cold Spring Harbor Symp. Quant. Biol.* **37** (1973).
6. H. E. Huxley, *Science* **164**, 1356 (1969).
7. E. B. Carew, I. M. Asher, H. E. Stanley, paper presented at the 9th International Symposium on Chemistry of Natural Products, Ottawa, 1974; in preparation.
8. I. M. Asher, E. B. Carew, H. E. Stanley, in *Physiology of Smooth Muscle*, E. Bülbiring, Ed. (Raven, New York, in press).
9. E. B. Carew, I. M. Asher, J. Gergely, A. Hewitt, J. Potter, J. C. Seidel, H. E. Stanley, in preparation.
10. K. J. Rothschild, I. M. Asher, E. Anastassakis, H. E. Stanley, *Science* **182**, 384 (1973); I. M. Asher, K. J. Rothschild, H. E. Stanley, *J. Mol. Biol.* **89**, 205 (1974); K. J. Rothschild and H. E. Stanley, *Science* **185**, 616 (1974).
11. I. M. Asher, G. D. J. Phillies, H. E. Stanley, *Biochem. Biophys. Res. Commun.* **61**, 1356 (1974); G. D. J. Phillies, I. M. Asher, H. E. Stanley, *Science*, in press.
12. M. C. Chen and R. C. Lord, *J. Am. Chem. Soc.* **96**, 4750 (1974).
13. T. J. Yu, J. L. Lippert, W. L. Peticolas, *Biopolymers* **12**, 2161 (1973).
14. R. C. Lord and N. T. Yu, *J. Mol. Biol.* **51**, 203 (1970).
15. ———, *ibid.* **50**, 509 (1970); M. C. Tobin, *Science* **161**, 68 (1968).
16. N. T. Yu, C. S. Liu, D. C. O'Shea, *J. Mol. Biol.* **70**, 117 (1972).
17. T. Miyazawa, T. Shimanouchi, S. Mizushima, *J. Chem. Phys.* **29**, 611 (1958).
18. K. M. Naus, S. Kitagawa, J. Gergely, *J. Biol. Chem.* **244**, 755 (1969).
19. S. Lowey and C. Cohen, *J. Mol. Biol.* **4**, 293 (1962).
20. E. W. Small, B. Fanconi, W. L. Peticolas, *J. Chem. Phys.* **52**, 4369 (1970).
21. L. Simons, G. Bergström, G. Blomfelt, S. Forss, M. Stenbäck, G. Wansén, *Commentat. Phys.-Math.* **42**, 125 (1972).
22. J. L. Lippert, personal communication.
23. We acknowledge stimulating conversations with and valuable advice of R. C. Lord, J. Gergely, J. C. Seidel, G. D. J. Phillies, K. J. Rothschild, J. Potter, and A. Hewitt. Supported by the Research Corporation, the National Science Foundation, and the National Heart and Lung Institute (grant HL 14322-03, R. W. Mann, principal investigator), and by NIH biochemical sciences support grant NIH-5-SO5-RR07047-08 to the Massachusetts Institute of Technology.

15 October 1974

***Pseudomyrmex nigropilosa*: A Parasite of a Mutualism**

Abstract. *Pseudomyrmex nigropilosa* is a parasite of the ant-acacia mutualism in Central America in that it harvests the resources of swollen-thorn acacias but does not protect the acacias. In the process, it also lowers the rate of occupation by the obligate acacia-ants, species of ants that do protect swollen-thorn acacias. Tenancy of an acacia by *P. nigropilosa* must be temporary, since the unoccupied plant is shortly killed by herbivores or competing plants, or is taken over by obligate acacia-ants. As expected of a species of short-lived ant, a *P. nigropilosa* colony produces reproductives earlier in the life of the colony and maintains fewer grams of workers per gram of brood than does a colony of the long-lived obligate acacia-ants.

In lowland Mexico and Central America there are 11 species of swollen-thorn acacias (*Acacia*). They are occupied by at least ten species of obligate acacia-ants (*Pseudomyrmex*); the worker ants patrol the surface of the acacias to keep off herbivores and vines, and in return the acacias produce food bodies and nesting structures. The ant colony cannot maintain itself away from the acacias, and in most habitats the acacias cannot survive to reproductive maturity without the services of

a colony of obligate acacia-ants (1-3). Here, I describe a widespread parasite of this mutualism and show how its colony structure is adjusted to a parasitic way of life.

Pseudomyrmex nigropilosa Emery is a yellow-red pseudomyrmecine ant with workers 6 to 8 mm long, a size similar to that of obligate acacia-ants (4). The workers cut their own entrance holes and nest exclusively in the thorns of swollen-thorn acacias (5), harvest the modified leaflet tips

as food bodies and feed them to their larvae just as do obligate acacia-ants, and obtain their sugars from the extrafloral nectaries on the acacia petiole. However, in very striking contrast to the obligate acacia-ants, the workers of *P. nigropilosa* do not protect the acacia against vines, insects, or vertebrates.

Pseudomyrmex nigropilosa neither attacks foreign objects on the acacia nor cleans its foliage of debris. When approached by an animal, the workers run behind the branches and often into a thorn. The workers are not active at night outside the thorns. In short, they behave toward foreign objects as do the workers of the many species of twig-inhabiting *Pseudomyrmex*, except that *P. nigropilosa* does not even scavenge moribund insects or catch small live ones. It is a true parasite of the coevolved system of aggressive obligate acacia-ants and swollen-thorn acacias. By occupying thorns and eating the food produced by the acacia, it lowers the rate of colonization by obligate acacia-ants and slows the growth of young obligate acacia-ant colonies. In turn, this interaction lowers the fitness of the acacia because, without protection from an obligate acacia-ant colony, it is more likely to die before maturity (2, 3).

How then does *P. nigropilosa* persist as such an extreme food specialist, since the acacia requires an aggressive, patrolling obligate acacia-ant colony to stay alive? A *P. nigropilosa* colony can survive as such a specialist because of the lag of as much as a year between the time when a swollen-thorn acacia loses its obligate acacia-ant colony and the time when it dies of herbivory or shading, or gains another obligate acacia-ant colony. Swollen-thorn acacias lose their usual occupants through fire, predation by birds, starvation of the colony through deciduousness of the acacia during an exceptional dry season, and unknown causes of queen death. The founding queens and colonies of *P. nigropilosa* sur-

Table 1. Three colonies of obligate acacia-ants (*Pseudomyrmex belti*, *P. ferruginea*, and *P. nigrocincta*) compared with one of *Pseudomyrmex nigropilosa* (11). All weights are oven dry.

Species	Workers			Alate virgins			Thorns on trees in colony		Physogastric queens (11) (N)		
	Total (g)	Per unit of brood (g/g)	Individual (mg)	Individual queen (mg)	Individual male (mg)	Total queens (g)	Total males (g)	Males/queens (g/g)		Total (N)	Percentage with brood
<i>P. nigrocincta</i>	5.67	0.84	0.48	1.06	0.55	0.9113	0.6454	0.708	1019	54	2
<i>P. ferruginea</i>	29.62	0.81	0.73	1.73	1.02	5.5443	1.4644	0.264	3488	46	1
<i>P. belti</i>	20.74	0.75	1.09	2.55	1.36	8.2256	5.4253	0.660	3131	51	1
<i>P. nigropilosa</i>	1.38	0.30	1.04	2.74	1.47	0.3099	0.2934	0.947	537*	59	11

* In addition to these, there were 230 thorns into which the *P. nigropilosa* workers had not bothered to cut entrance holes, which suggests that they are limited by food, not space. All food bodies had been harvested from the leaves of the swollen-thorn acacia occupied by this colony.